This is a repository copy of *On the use of a fictitious notch radius equal to 0.3 mm to design against fatigue welded joints made of wrought magnesium alloy AZ31*.

Article:

On the use of a fictitious notch radius equal to 0.3 mm to design against fatigue welded joints made of wrought magnesium alloy AZ31

Özler Karakaş [a*], Jörg Baumgartner [b], Luca Susmel [c]

[a] Department of Mechanical Engineering, Faculty of Engineering, Pamukkale University, 20160 Kinikli, Denizli, Turkey
[b] Fraunhofer Institute for Structural Durability and System Reliability LBF, 64289 Darmstadt, Germany
[c] Department of Civil and Structural Engineering, the University of Sheffield, Sheffield S1 3JD, UK

* Corresponding author

Abstract

In the present investigation, a large number of fatigue data generated by testing welded joints of magnesium alloy AZ31 were post-processed based on the reference radius concept. The local stresses used to perform this systematic re-analysis were determined by setting the fictitious notch radius, r_f, invariably equal to 0.3 mm. According to this strategy, local stress-based S-N curves were then derived for load ratios, R, equal to -1, 0 and to 0.5. This post-processing exercise allowed us to demonstrate that a fictitious notch radius of 0.3 mm is successful in modelling the fatigue strength of weldments made of magnesium alloy AZ31. In particular, with $r_f = 0.3$ mm, this type of welded joints is recommended to be designed against fatigue by using an S-N curve having endurable local stress range, $\Delta\sigma_{FAT}$, at $N = 2 \times 10^6$ cycles to failure equal to 40 MPa and a negative inverse slope, k, equal to 3.

Keywords: welded joints; magnesium alloy; local stress; fictitious radius; fatigue design

Nomenclature

r_f	Fictitious notch radius
R	Load ratio
t	Thickness
ρ^*	Microstructural length
K_t	Stress concentration factor
σ_{eff}	Fatigue effective stress
L	Material length scale
r_{real}	Real notch radius
s	Support factor
k	Slope of S-N curves before knee point
k^*	Slope of S-N curves after knee point
T_σ	Scatter value
$\sigma_{n,a}$	Nominal stress amplitude
$\Delta\sigma_{loc}$	Local equivalent stress range
P_s	Probability of survival
P_c	Confidence level
$\sigma_{n,m}$	Nominal stress amplitude
j_σ	Safety factor
$\Delta\sigma_{5E5}$	Endurable stress range
$\Delta\sigma_{FAT}$	FAT-value
$\Delta\sigma_{e,C}$	Endurable characteristic normal stress range

1. Introduction

As far as the fatigue behaviour of welded joints is concerned, the locations of highly damaged regions with respect to weld geometries and stress distributions indicate a clear correlation between fatigue damage extent and local values of stresses and strains. This explains the reason why local approaches have become increasingly more important in the past decade in fatigue studies of welded joints, especially along with the development of more powerful

computational tools for Finite Element (FE) analysis. Although the local concepts are not a recent development, owing to its flexibility and reliability, this simple design approach is certainly one of the most widely used in situations of practical interest for fatigue assessment of welded connections [1-6].

In addition to the notch stress concepts, which includes fictitious notch radius [7-12] used in the current paper, local approaches consists of many different methods which generally assume local parameters such as local stress and local strain to be relevant to the fatigue behaviour of the material and has been reported successful on many different publications with structural stress [13,14] and structural strain concepts [15,16], fracture mechanics concepts such as extended stress intensity factor (SIF) concepts [17,18] and local strain energy density (SED) methods [19-24].

Amongst the local approaches being developed and validated so far, the fictitious radius concept is known for its wide and straightforward applicability. Depending on the thickness of the welded joint and the type of material, weld toes and weld roots can be modelled by using different fictitious notch radii. For steel plates with thickness, t, larger than 5 mm, a fictitious notch radius, r_f, equal to 1 mm is recommended in the design guidelines of the International Institute of Welding (IIW) [25]. This value can also be used to assess the fatigue strength of aluminium welded joints [26-29]. In contrast, as demonstrated in Refs [28-30], a fictitious notch radius of 0.05 mm is always recommended to be used to assess steel and aluminium welded connections with thickness lower than 5 mm. Further, regardless of the type of welded geometry [31,32], $r_f = 1$ mm and $r_f = 0.05$ mm are used also for magnesium welded joints with $t \geq 5$ mm and $t < 5$ mm, respectively. In this context, it is worth mentioning also that the reference radius concept is seen to be successful also in designing welded joints against multiaxial fatigue [33].

In recent years, a value of the reference radius equal to 0.3 mm has been introduced for steel and aluminium welded joints with plate thickness, t, varying in the range 3 mm-10 mm [34]. In this setting, several investigations [35-39] have demonstrated the applicability of the $r_f = 0.3$ mm approach for steel and aluminium welded joints, with these studies showing that, compared to the $r_f = 0.05$ mm solution, less conservative results are obtained with thin connections.

According to Refs [40, 41], based on the formula linking the fictitious notch radius with Neuber's microstructural length ρ^* [42], a reference value for r_f of 0.3 mm was calculated also for welded joints made of magnesium alloy. This fictitious notch radius clearly coincides with the third possible value being recommendation to design both steel and aluminium welded joints with plate thickness in the range 3mm-10mm [34]. However, in Refs [40, 41] the problem of the fatigue assessment of magnesium welded joints based on the $r_f = 0.3$ mm concept was not studied in depth not to lose the focus on the specific aims of those investigations. To fill this knowledge gap, the present work aims then at demonstrating the applicability of a fictitious notch radius, r_f, equal to 0.3 mm also to the fatigue assessment of magnesium welded joints. Accordingly, to the best of the authors' knowledge, this paper summarises the first systematic attempt to model and assess the fatigue behaviour of magnesium welded joints by setting r_f equal to 0.3 mm. To this end, a large number of fatigue data were selected from the technical literature, with these experimental results being generated by testing welded joints made of magnesium alloy AZ31. The fatigue results being re-analysed were obtained by testing three different weld geometries (i.e., transverse full/partial penetration butt welded connections and joints with transversal stiffener) under three different values of the stress ratio (i.e., R=-1, R=0 and R=0.5). The stress concentration factors (K_t) at the weld toes were recalculated based on $r_f = 0.3$ mm. Finally, the obtained local stresses allowed the experimental data to be summarised using suitable S-N design curves.

2. Theoretical Background

In order to model in the presence of a notch the effect, under cyclic loading, of the stress field gradient - defined as $\sigma(x, y, z)$, several methods have been proposed over the years. In this setting, the fatigue effective stress, σ_{eff}, can be evaluated from the stress field and used in non-local fatigue assessments. Neuber's stress averaging method [42] and the Point Method [43, 44] focus on calculating this effective stress which is seen to be proportional to the extent of fatigue damage.

In Neuber's stress averaging method, the effective stress is calculated by determining the stress distribution at the notch root over a microstructural length ρ^* [42].

$$\sigma_{eff} = \frac{1}{\rho^*} \int_0^{\rho^*} \sigma_1(x) dx \tag{1}$$

Turning to the Point Method, a fictitious point along the stress distribution path, $\sigma(x)$, at the notch root is considered. The stress at this point corresponds to the effective stress and the distance to this fictitious point is the critical distance "a" [43, 44]. The relation between critical distance and effective stress can be formulised as:

$$\sigma_{eff} = \sigma_1(x = a) \tag{2}$$

A schematic representation of these two methods is provided in Figure 1. As it can be deduced, both microstructural length ρ^* and critical distance a can be used to determine the effective stress as long as the stress distribution in the vicinity of the notch tip can be determined unambiguously. In this context, the relevant stress distributions are usually determined via conventional linear-elastic FE analyses.
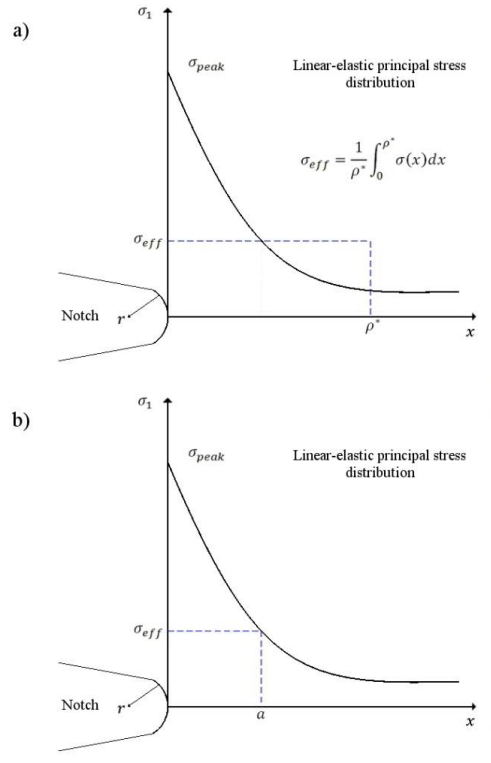
Figure 1: Schematic representation of Neuber's stress averaging method (a) and the Point Method (b) [41].

Both microstructural length ρ^* and critical distance a are material-dependent parameters. The correlation between these two lengths were also established in Ref. [44]. This allowed these two methods to be grouped together under a unifying umbrella, with this umbrella being named by our colleague Professor David Taylor as the Theory of Critical Distances (TCD). In particular, the TCD includes Neuber's stress averaging method which is referred to as the Line Method (LM), the Point Method (PM), the Area Method and, finally, the Volume Method [45]. Further, it was also derived an equation to establish a link amongst material length scale L, microstructural length ρ^*, and critical distance a, i.e.:

$$L = \frac{\rho^*}{2} = 2a \qquad\qquad (3)$$

The value of the fictitious notch radius is based on Neuber's microstructural support theory [42] which establishes a relationship between fictitious notch radius r_f and microstructural length ρ^*. This relationship can be expressed explicitly as follows:

$$r_f = r_{real} + s \cdot \rho^* \qquad\qquad (4)$$

where r_{real} is the real notch radius and s is a support factor. The support factor s depends on multitude of conditions, as reported in [9,10,11] which include loading mode 1,2,3, mixed mode loading, multiaxiality condition of the notch tip and applied strength criterion. Additionally, opening angle of the notch and shape of the notch were determined to affect the support factor significantly. Although this complicated dependency may seem to counteract the claimed simplicity of fictitious notch radius, by considering "worst-case scenarios" value of support factor s can be approximated.

The relationship between r_f and r_{real} as expressed by Eq. (4) is also shown schematically in Figure 2. According to Eq. (4) and Figure 2, the fictitious notch radius is expected to be larger than the real notch radius, resulting in lower local fictitious stresses. This allows less conservative fatigue assessment to be performed. However, it is worth noting that the real notch radius, r_{real}, is often taken invariably equal to zero (sharp notch) in order to assume aforementioned the worst-case scenario in the calculations.
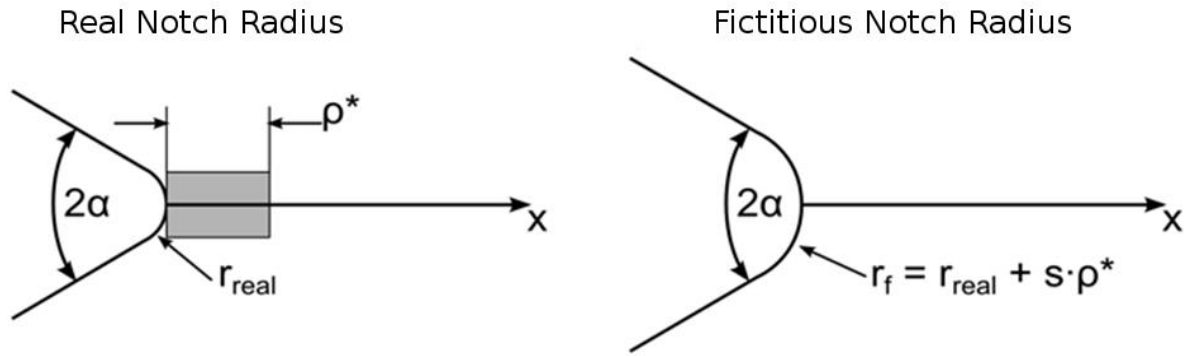
Figure 2: According to Neuber [42], relationship between real notch radius and fictitious notch radius [46] (modified).

As far as weldments are concerned, a fictitious notch radius of 1 mm was derived using Eq. (4) ($r_{real} = 0$, $s = 2.5$ and $\rho^* = 0.4$ for steel) [42] and is applicable to welded joints of steel, aluminium and magnesium plates with thicknesses $t \geq 5$ mm. On the other hand, $r_f = 0.05$ mm was derived based on fracture mechanics considerations instead of Eq. (4) [47-49] and is applicable to welded joints of steel, aluminium and magnesium plates with thicknesses $t < 5$ mm.

3. Determination of notch stresses

The experimental data used in this study were taken from the technical literature and were all generated by testing magnesium welded joints. Detailed information regarding the experimental procedure being adopted can be found in Ref. [50]. In order to clearly show the geometries of the welded specimens being consider, the corresponding technical drawings and pictures are reported in Figure 3.
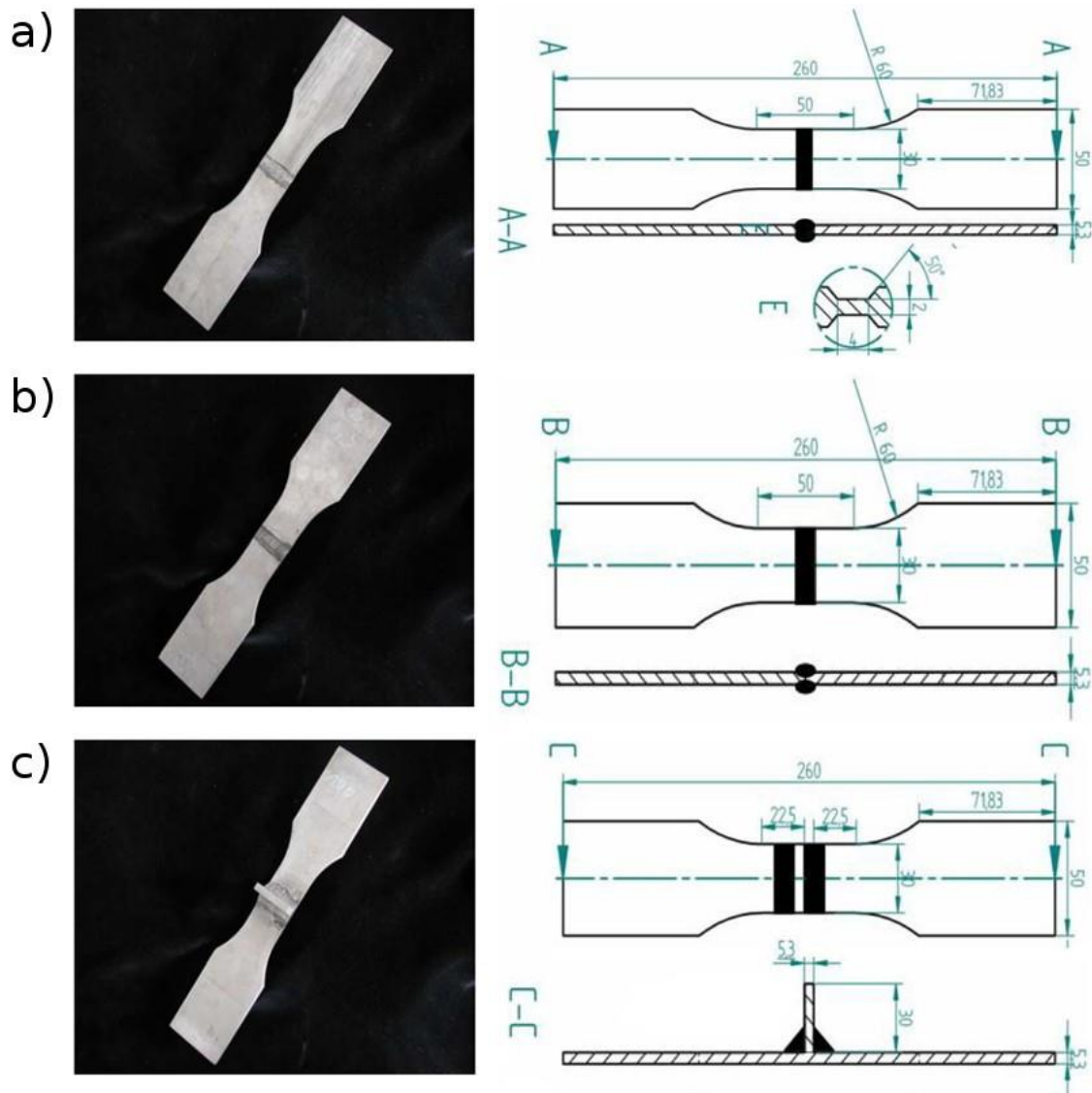
Figure 3: Pictures and technical drawings of the welded specimens being considered: transverse full penetration butt welded (a), transverse partial penetration butt welded joint (b), and transversal stiffener (c) [50].

Further, in order to broaden the available data sets, laser-beam welded tube-tube specimens made from the same magnesium alloy [51] with a sheet thickness, t, of 1.5 mm were also included in the re-analyses being presented in what follows.

FE models of the welded geometries being considered were solved in order to determine the corresponding stress distributions and notch stress concentration factors. Thus, for each geometry being re-analysed, the local linear-elastic stresses were calculated directly from nominal stresses and then summarised in suitable S-N curves.

The FE analyses were run as follows [31]:

- 2D quadratic elements with 8 nodes;

- quadratic function for the displacement of the nodes;

- linear stress and strain function within the elements;

- plane strain conditions;

- uniform displacement distribution applied at the extremity;

- highly stressed area meshed with elements having dimensions equal to r/20, where r is the notch radius.

For any considered welded geometry, 1 MPa nominal stress was used as loading boundary condition. Some examples of the FE models that were solved are seen in Figures 4-6.
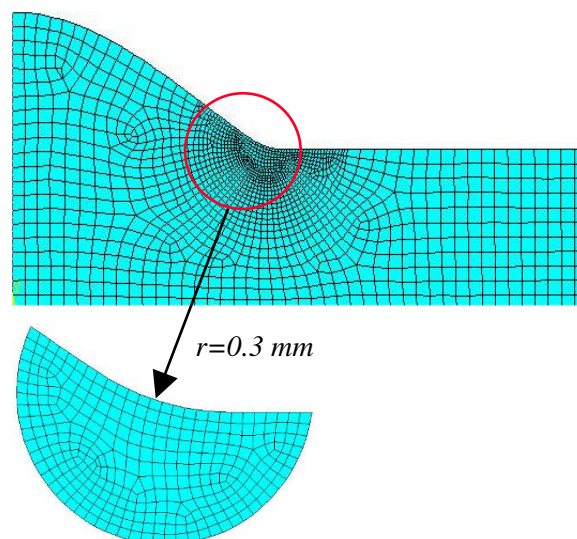

r=0.3 mm

Figure 4: FE model of fully penetrated butt-welded specimen.
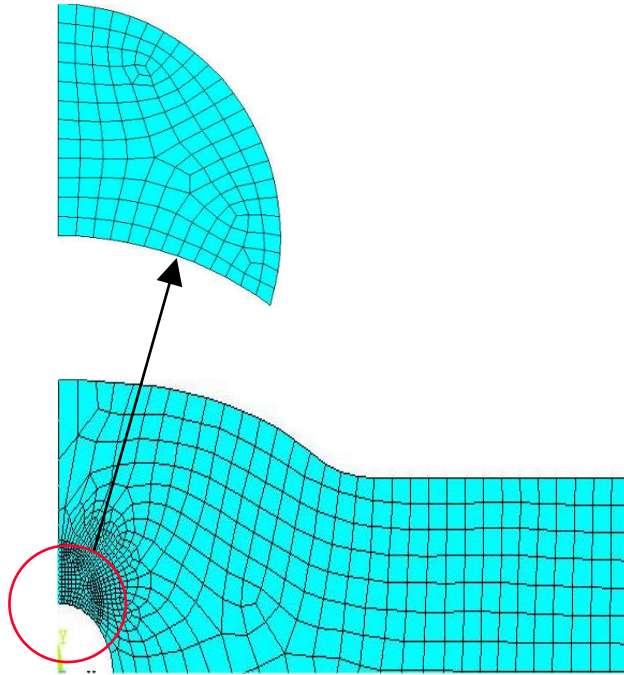
Figure 5: FE model of non-fully penetrated butt-welded specimen.
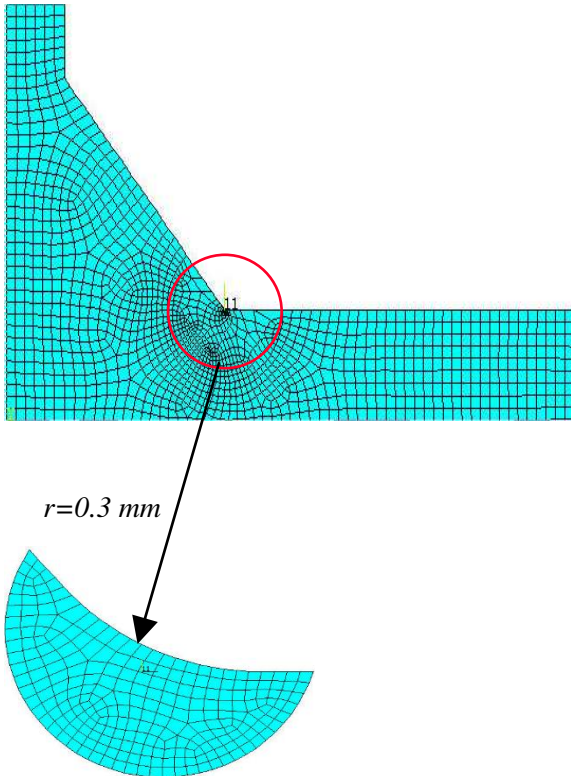

r=0.3 mm

Figure 6: FE model of transversal stiffener specimen.

In addition to the FE analyses, stress concentration factors were also calculated based on analytical equations suitable for assessing the specific welded geometries under investigation. For full penetration butt welded connections, the solutions proposed by Lawrence and Yung [52], Eq. (5), and by Anthes [53], Eq. (6), were used, i.e.:

$$K_t = 1 + 0.27 \cdot (\tan \theta)^{0.25} \cdot \left(\frac{t}{\rho}\right)^{0.5} \tag{5}$$

$$K_t = 1 + 0.728 \cdot (\sin \theta)^{0.932} \cdot \left(\frac{t}{\rho}\right)^{0.382} \tag{6}$$

In contrast, for partial penetration butt welded joints, the solution proposed by Lehrke was employed [54, 55]:

$$K_t = 1 + \frac{2}{\sqrt{\cos\left(\frac{\pi}{2} \cdot \frac{s}{t}\right)}} \cdot \sqrt{\frac{s}{2\rho}} \tag{7}$$

Finally, for welded joints with transverse stiffeners, the analytical formula, Eq. (8), derived by Anthes [53] was used, with the values of the relevant coefficients being reported in Table 1:

$$K_t = m_0 + \left(1 + m_2 \cdot \left(\frac{t}{r}\right)^{p3} + m_3 \cdot (\sin(\theta))^{p4}\right) \cdot (\sin(\theta))^{p5} \cdot \left(\frac{t}{r}\right)^{p6} \tag{8}$$

Table 1: Coefficients used in Eq. (8) for the stress concentration factor calculations of transversal stiffeners.

	m_0	m_2	m_3	p3	p4	p5	p6
Tension	1.538	1.455	-2.933	0.208	1.213	2.086	0.207
Bending	1.256	2.153	-3.738	0.154	0.481	1.723	0.172

Comparison between the values of the stress concentration factors determined both from the FE analyses and from the analytical solutions are presented in Figures 7-9 for each welded

geometry being considered. In general, it can be observed that both methods for calculating the stress concentration factors resulted in markedly consistent values. In particular, for fully penetrated (Figure 7) and partially penetrated (Figure 8) butt welds, the stress concentration factors from the analytical calculations were seen to be lower than the corresponding values from the FE analyses. In contrast, for the transversal stiffeners, the K_T values from the FE analyses were seen to be much higher than the corresponding values from the analytical calculations (Figure 9).
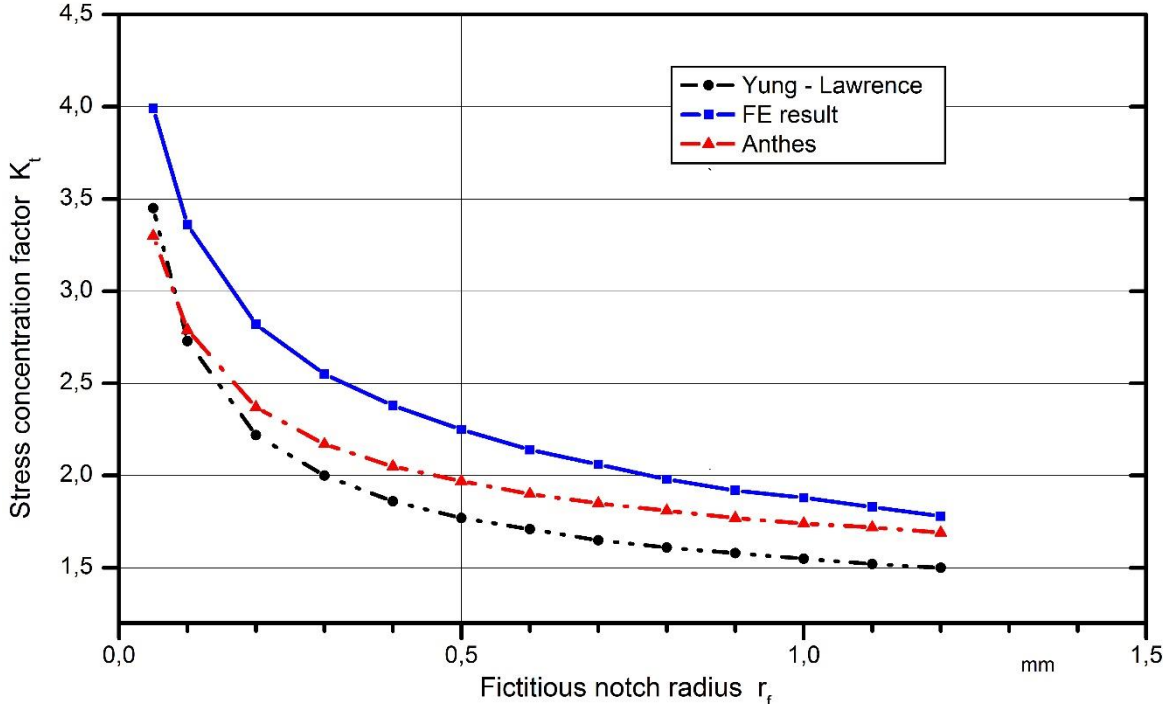

Figure 7: Comparison of stress concentration factors of fully penetrated butt welds based on analytical equations and FE analysis.
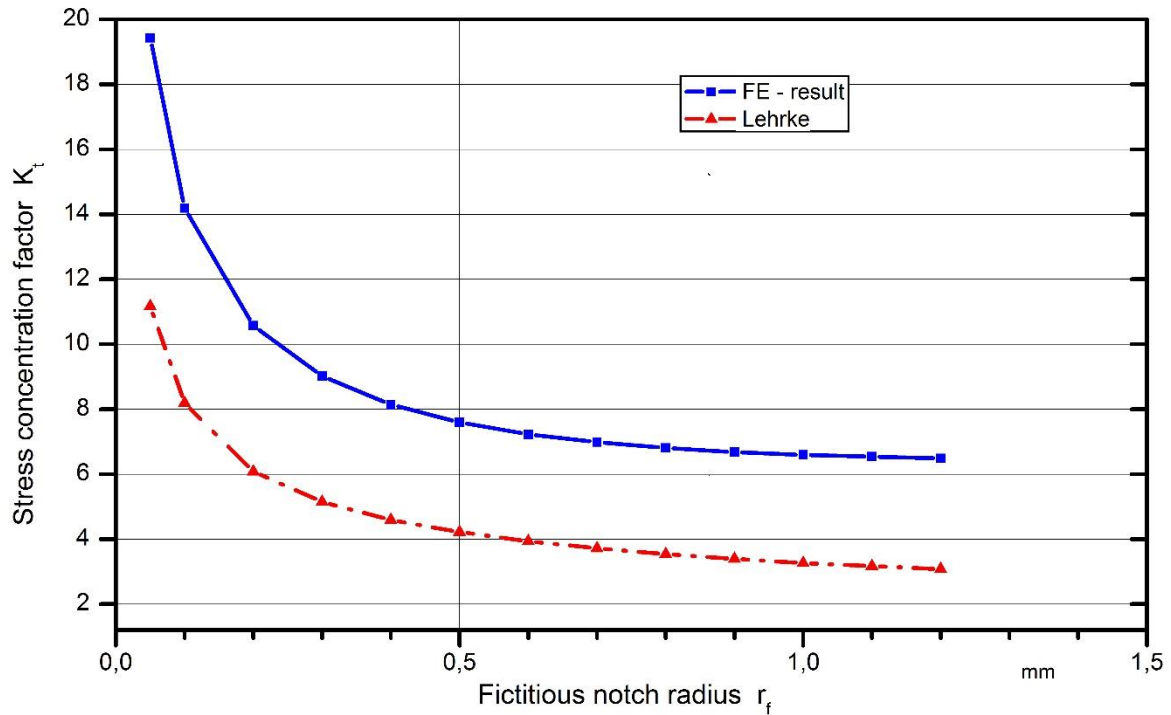
Figure 8: Comparison of stress concentration factors of non-fully penetrated butt welds based on analytical equations and FE analysis.
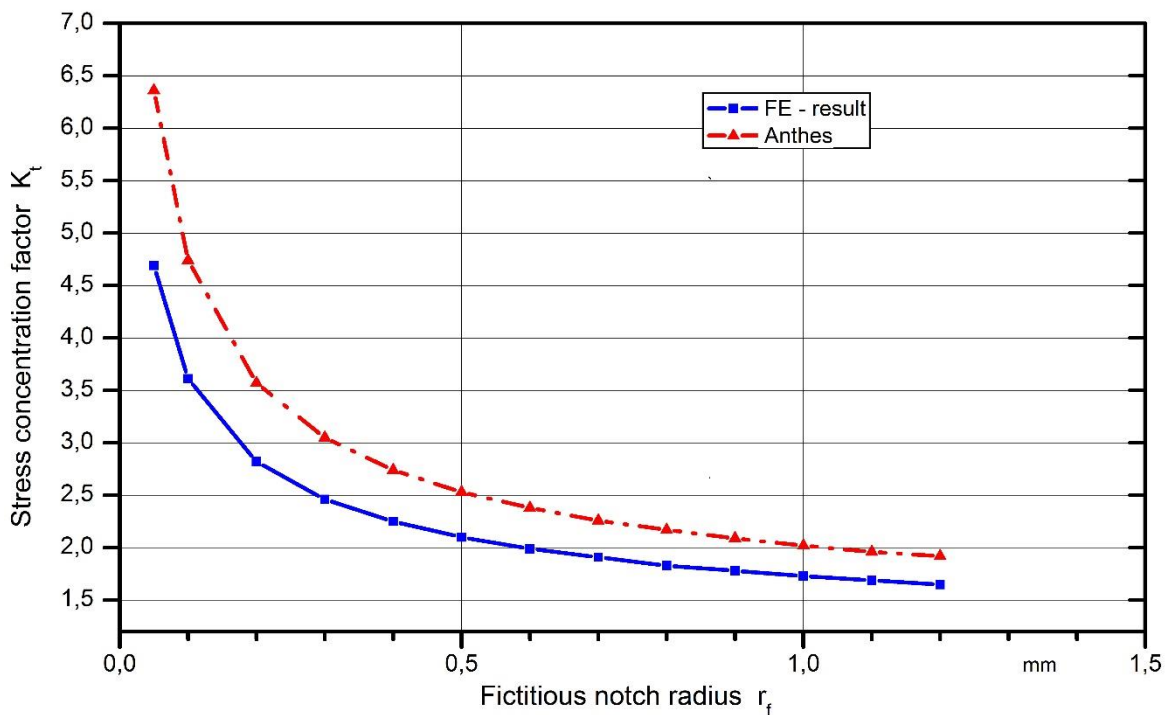

Figure 9: Comparison of stress concentration factors of transversal stiffeners based on analytical equations and FE analysis.

Based on the FE models being solved, the notch stress concentration factors for each welded geometry were then calculated for different values of the fictitious notch radius, with the obtained results being listed in Table 2.

Table 2: FE analysis results of stress concentration factors for each welded geometry being investigated based on the fictitious notch radius concept.

Fictitious notch radius r_f [mm]	Stress concentration factor K_t			
	Fully penetrated	Non-fully penetrated	Transversal stiffener	Overlapping tube
0.05	3.99	19.43	4.69	61.04
0.10	3.36	14.19	3.61	47.92
0.20	2.82	10.57	2.82	39.78
0.30	2.55	9.02	2.46	37.48

Since overlapping tube-tube welded specimens with $t = 1.5$ mm were thinner than the butt joints and transversal stiffeners with $t = 5.3$ mm, only notch stresses up to $r_f = 0.3$ mm were calculated since the calculated stresses becomes unreliable once the reference radius is larger than one fifth of the wall thickness ($r_f > 0.2 \cdot t$) [36]. This is due to the fact that, given the cross-section wall thickness of the sample, a larger fictitious radius would weaken the cross section, leading to wrong estimated of the stress state in the weld.

In addition, Figure 10 explicitly shows how the stress concentration factors vary as the value of the fictitious notch radius changes.
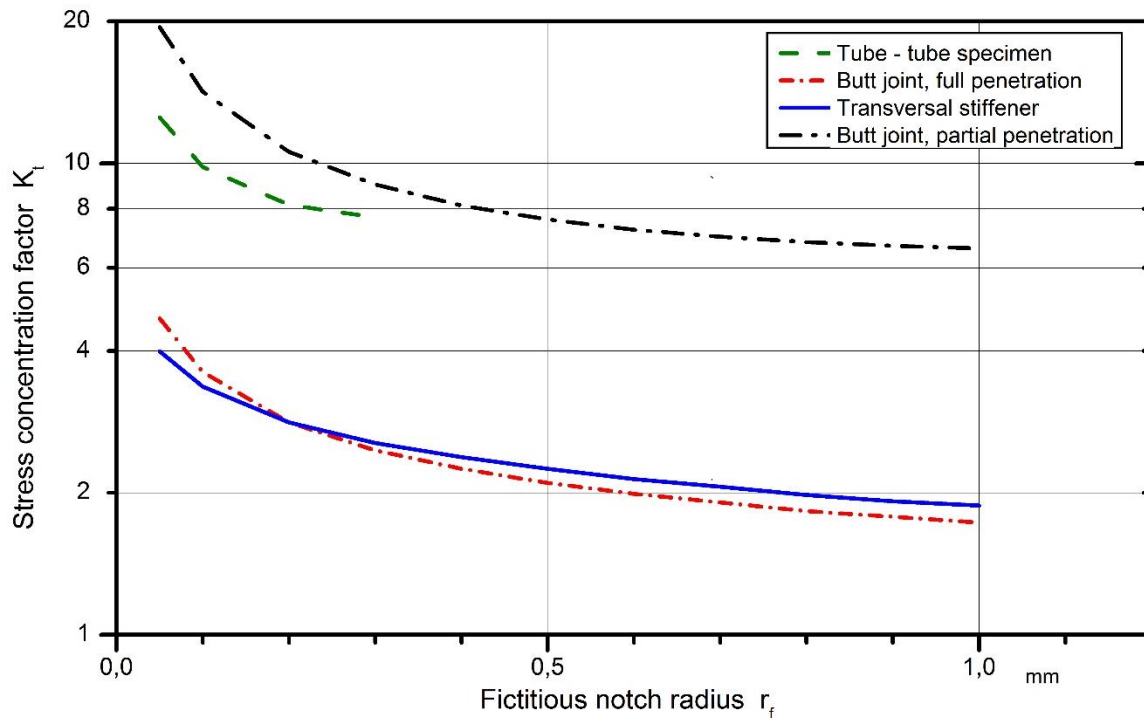
Figure 10: Change in stress concentration factors in relation to fictitious notch radius.

Numerical calculations based on FE models assume a 2D-model instead of 3D. As expected, this difference in models create a discrepancy in results. However, difference in principal stress of 2D and 3D-models of sharply notched specimens are only between 1%-3%. Thus, application of the method using 3D-models would not create a meaningful difference that can justify the added complexities in modelling of the notch and calculations.

4. Results and Discussions

As mentioned earlier, the experimental results being re-analysed were discussed in detail in references [50, 51] solely in the nominal stress system. For the sake of completeness and clarity, a summary of these fatigue test results in terms of nominal stress amplitudes at $N = 5 \times 10^5$ and $N = 5 \times 10^6$ is presented once again in Table 3 for each welded geometry. The negative inverse slope of the nominal S-N curves was seen to be equal to 3 (i.e., k=3) before and equal to 22 (i.e., $k^* = 22$) after the knee point, with the knee point being taken at 5×10^5 cycles to failure. These values were determined in accordance with the expected course of the S-N curves

16

[56]. It should also be noted that all the test results in terms of nominal stresses were seen to fall within a uniform scatter band with a scatter value, T_σ, of $1:1.40$.

Table 3: Fatigue parameters in terms of nominal stress amplitudes for different stress ratios at $N = 5 \times 10^5$ and $at\ N = 5 \times 10^6$ cycles to failure.

Material	Stress ratio	Fully penetrated butt weld		Partially penetrated butt weld		Transversal stiffener	
		$\sigma_{n,a(5E5)}$ [MPa]	$\sigma_{n,a(5E6)}$ [MPa]	$\sigma_{n,a(5E5)}$ [MPa]	$\sigma_{n,a(5E6)}$ [MPa]	$\sigma_{n,a(5E5)}$ [MPa]	$\sigma_{n,a(5E6)}$ [MPa]
Magnesium AZ31	R = -1	25	22.5	8	7.2	40	36
	R = 0	18	16.2	6	5.4	27	24.3
	R = 0.5	15	13.5	5	4.5	18	16.2

For each stress ratio, the values of the local stresses calculated numerically were used to plot the corresponding local S-N curves which are provided in Figures 11, 12 and 13 for R=-1, R=0 and R=0.5, respectively. In these diagrams, the results from all the welded geometries are summarised in the local stress system by adopting unified scatter bands having slope, k, equal to 3. Additionally, also the scatter values, T_σ, are reported for each local S-N curve.
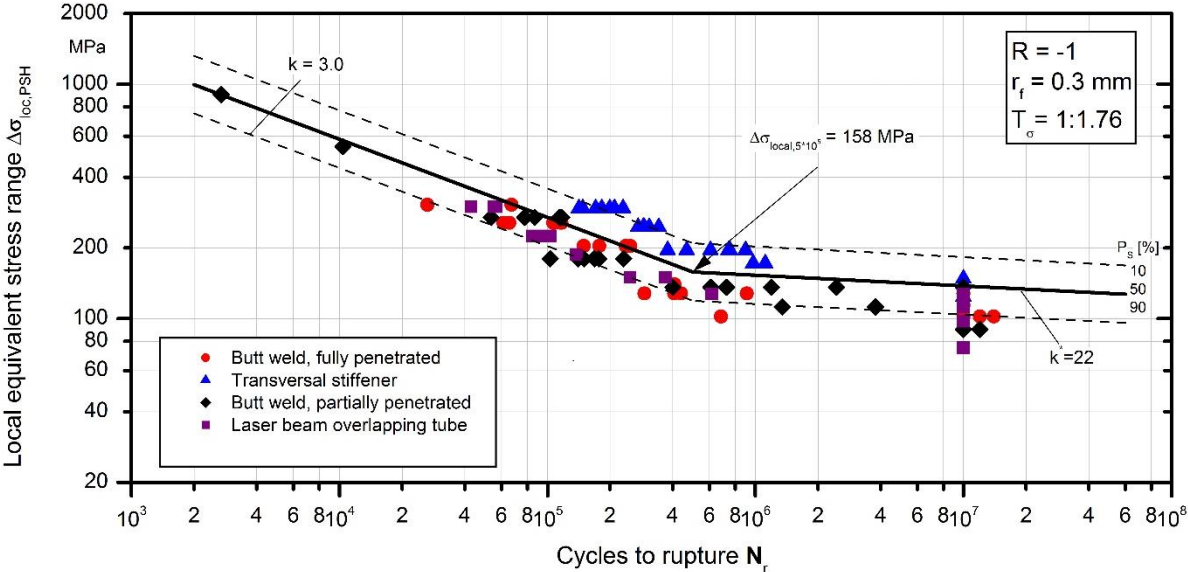
Figure 11: Local S-N curve for a fictitious notch radius, r_f, equal to 0.3 mm under R=-1.
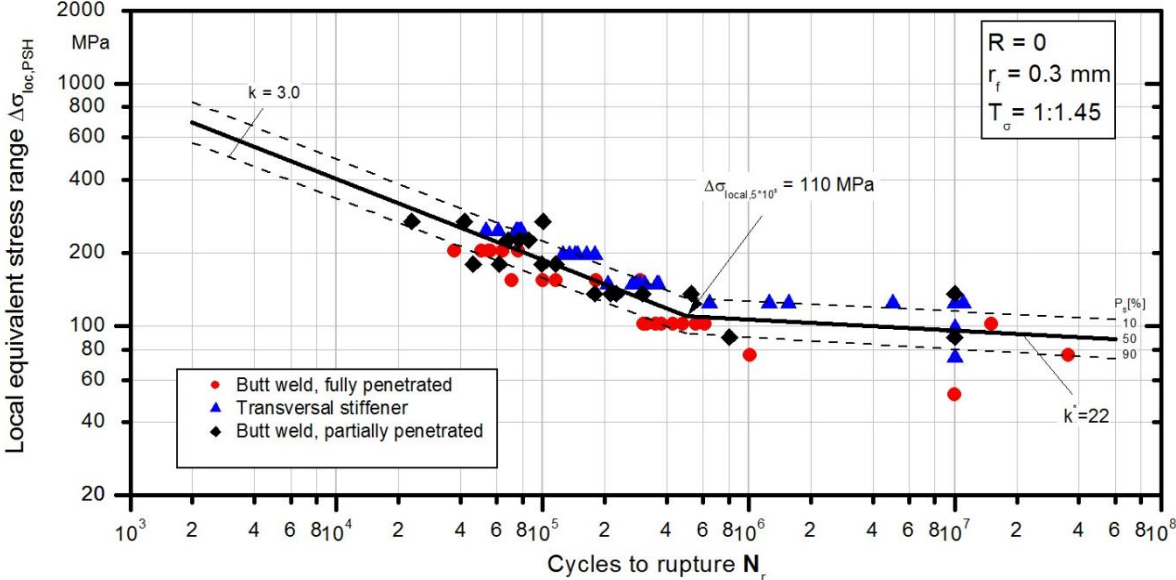

Figure 12: Local S-N curve for a fictitious notch radius, r_f, equal to 0.3 mm under R=0.
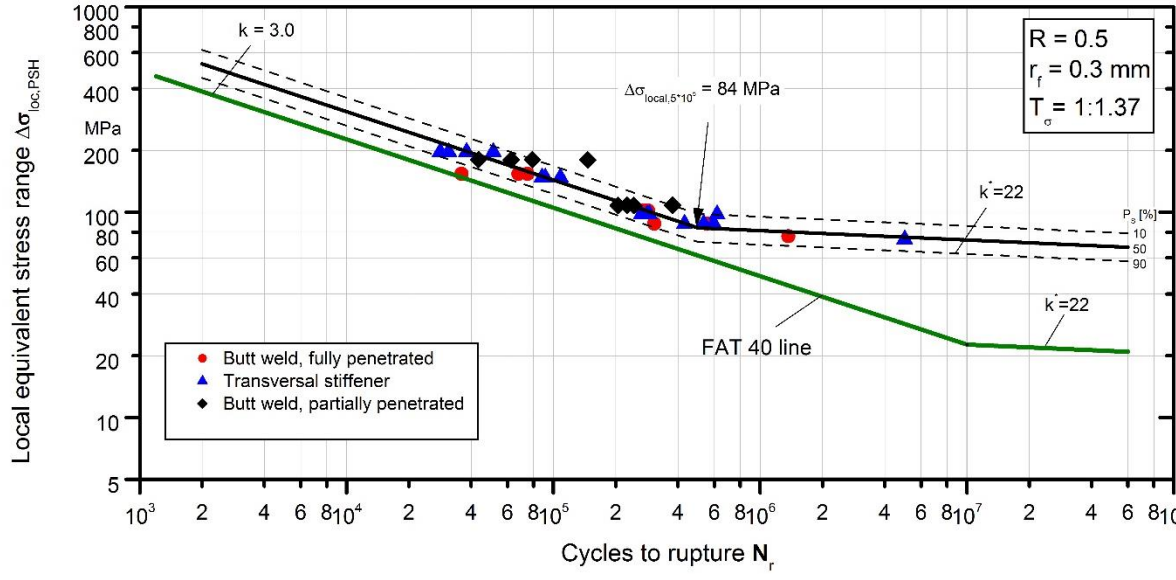

Figure 13: Local S-N curve for a fictitious notch radius, r_f, equal to 0.3 mm under R=0.5.

The statistical correlation between fictitious notch radius r_f and the scatter values $T_\sigma^* = 1$:

$T_\sigma = [\sigma(P_s = 10\%)/\sigma(P_s = 90\%)]$ are shown in Figure 14 for stress ratios R=-1, R=0 and

R=0.5 [31]. The minimum scatter value for each stress ratio is seen to be between $r_f = 0.6$ mm

and $r_f = 1.0$ mm. In the evaluation of the scatter for R = -1, the tube-tube specimens were

included up to a reference radius of $r_f = 0.3$ mm and the scatter values of tube-tube specimens

appear to agree well with the scatter of other welded specimens up to this point. For reference

radii larger than $r_f = 0.3$, tube-tube specimens do not return meaningful scatters due to a

significant reduction in the specimens' wall thickness. Outside of this area, the scatter values

steadily increase especially below $r_f = 0.2$ mm. Therefore, it can be deduced that for r_f values

below 0.3 mm, the local notch effect associated with the weld seams can be approximated by

using the stress concentration factors calculated via the FE models made by introducing notch

radius r_f. Additionally, an increase in the scatter values when adopting smaller fictitious

reference radii is a phenomenon that was observed also in aluminium [27] as well as in steel
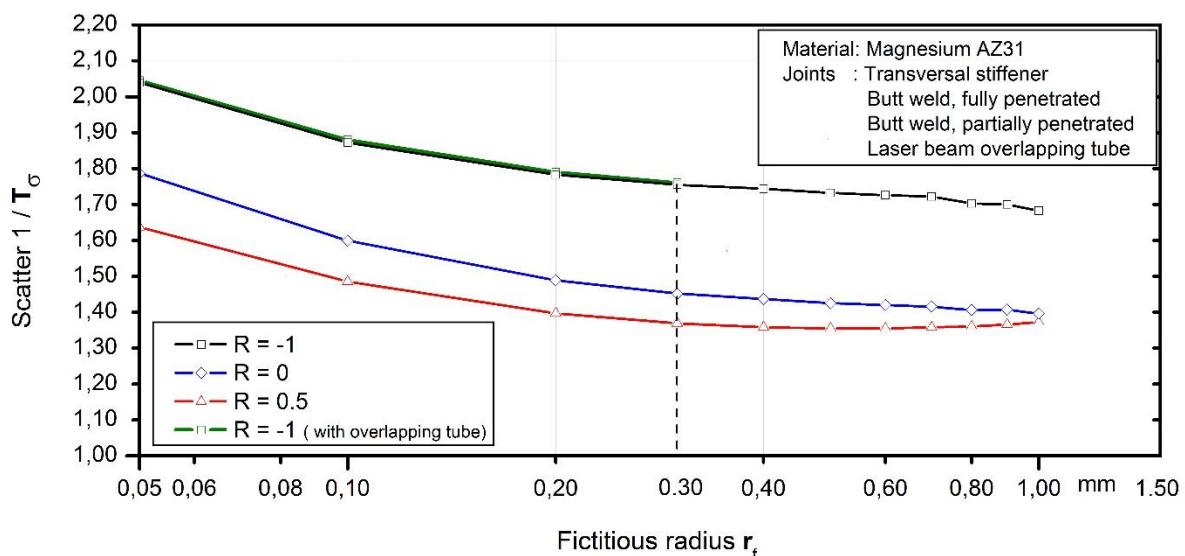
welded joints [36].

Figure 14: Changes in scatter values based on fictitious notch radius for each stress ratio [31] (modified).

As the fictitious notch radius r_f decreases, the notch effect due to the weld seams approaches the sharp notch behaviour and the scatter values increase. As for very large values of r_f, the presence of the fictitious rounded notch weakens the specimen, with this leading to simulations that do not capture accurately the mechanical behaviour being modelled (Figure 10). Additionally, the correlation between geometry of the weld and variations in stress concentration factor values is worth being mentioning. In particular, for welded geometries with higher stress concentration factors, a decrease in r_f causes a more significant increase in the stress concentration factor.

As far as the scatter values are concerned, another aspect to be considered is the effect of the stress ratios. In order to explain the marked increase in scatter values for R=-1, Haigh diagrams of the weld geometries should be observed, which are provided in Figure 15. Scatter increases as a result of minor imperfections caused by the welding process and this effect is observed to be more prominent under fully-reversed loading (R=-1) compared to the other loading ratios (R=0 and R=0.5). The secondary stresses created by the welding imperfections are superposed during fatigue loading. Under fully-reversed loading, these secondary stresses create a wider range of variation in the local stresses, with this resulting also in a variation of the local stress ratios in the range -2÷0 [31]. Therefore, fully-reversed loading causes higher mean-stress sensitivity. This can also be observed from the steeper slope of the Haigh curves under R=-1 in comparison to the Haigh curves under R=0 and under R=0.5. However, it should be noted that individual scatters of different stress ratios do not influence the reference S-N curves significantly.
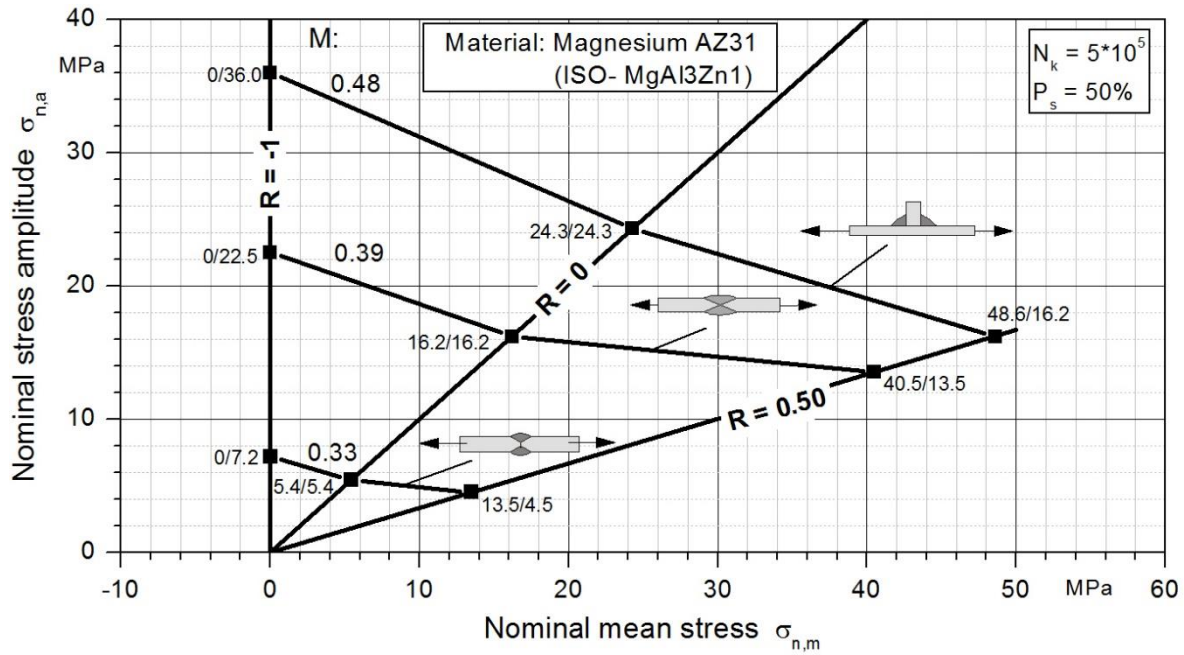
Figure 15: Haigh diagram for weld geometries [40].

As recommended by the IIW [25,57], in order to present design S-N curves for magnesium welded joints making use of a fictitious notch radius equal to 0.3 mm, the local stress values were derived for a probability of survival P_s equal to 97.7%, a confidence level P_c equal to 95%, and stress ratio, R, equal to 0.5. Based on these assumptions, $\Delta\sigma_{FAT} = 40$ MPa was calculated at $N = 2 \times 10^6$ cycles to failure.

By considering a scatter value of $T_\sigma = 1:1.50$ and a Gaussian log-normal distribution, values for $P_s = 97.7\%$ were obtained by reduction of the experimental values with $P_s = 50\%$ by safety factor $j_\sigma = 1.37$ [31]. For each stress ratio, the resulting reference S-N curves are provided in Figure 16. In addition, local stress ranges are provided in Table 4 for $P_s = 50\%$ and $P_s = 97.7\%$. The latter can be used as design S-N curve for welded magnesium structures. It should be noted that $r_f = 0.3$ mm is not yet part of the IIW-Recommendations. Considering the worst-case scenario, the S-N curve presented in Figure 17 is proposed and can be summed

up as follows. S-N curves should be plotted with endurable local stress range of $\Delta\sigma_{5E5} = 61$ MPa for R=0.5 at $N = 5 \times 10^5$ with $P_s = 97.7\%$ and slope of $k = 3.0$ up to $N = 1 \times 10^7$ cycles. The stress range of $\Delta\sigma_{FAT} = 40$ MPa at $N = 2 \times 10^6$ can be used as FAT-value. For cycles higher than $N = 1 \times 10^7$, a local stress range of $\Delta\sigma_{1E7} = 22$ MPa, where, after the knee point, a slope of $k^* = 22.0$ and of $k = 5.0$ should be used for constant amplitude loading and for variable amplitude loading, respectively.

Table 4: Endurable local stress ranges for magnesium welded joints based on $r_f = 0.3$ mm at $N = 5 \times 10^5$.

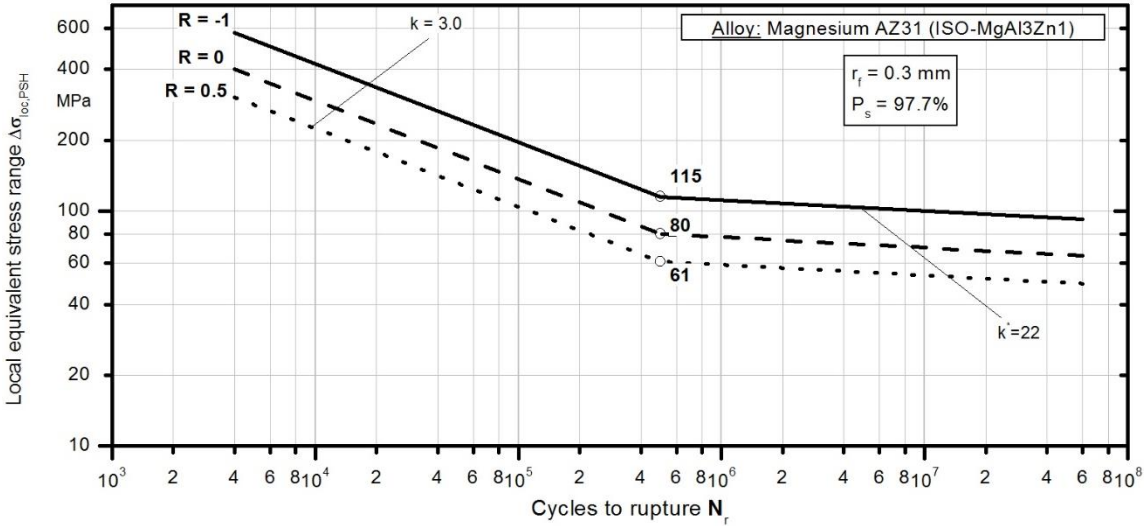| Stress ratio R	Local stress range ($P_s = 50\%$) [MPa]	Endurable local stress range ($P_s = 97.7\%$) [MPa]
-1	158	115
0	110	80
0.5	84	61

Figure 16: Reference S-N curves for fictitious notch radius $r_f = 0.3$ mm ($P_s = 97.7\%$).
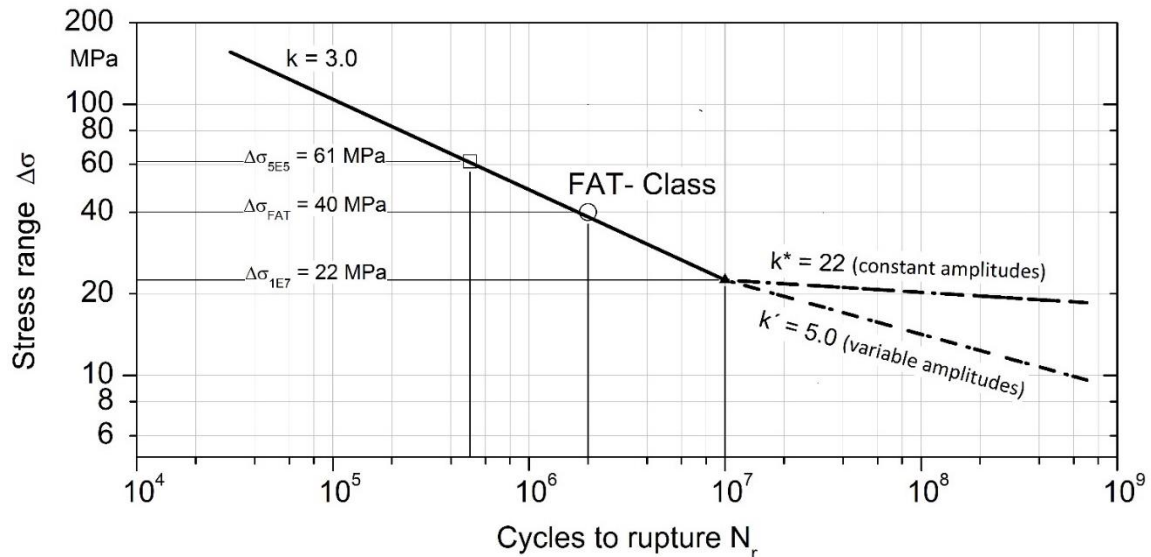
Figure 17: Suggested S-N curve for the IIW-Recommendations based on fictitious notch radius $r_f = 0.3$ mm.

In a recent work [31], FAT-values for magnesium alloys have been recommended for the reference radii $r_{ref} = 1$ mm (FAT28) and $r_{ref} = 0.05$ mm (FAT73). In the current investigations, a FAT-value of FAT40 has been identified. Based on empirical data and theoretical considerations [39][39] a power function between the radius and the (endurable) notch stress is expected. This is also the result for magnesium welded joints, Figure 18.

Theoretically [39], there should be a difference in the endurable stress between weld toe and weld root failure. For weld root failures, higher endurable stresses are expected since the stress gradients at notches with a weld opening angle smaller than 90° are comparatively steep. This leads to a high gradient-based support effects. When maximum notch stresses are evaluated, these support effects are not going to be considered directly, e.g. by the stress averaging or critical distance approach, but lead to higher endurable stresses in the case of sharp notches.

However, this expectation cannot be met since the partial penetration butt joint with the sharp root notch has the highest stress concentration (and subsequently the highest stress gradients) but lies in the middle of the scatter band for the evaluation with $r_{ref} = 1.0$ mm [31] and $r_{ref} =$

23

0.05 mm [41][41]. Also, for the evaluation with the radius $r_{ref} = 0.3$ mm no such tendency can be identified, Figure 14.

A reason for this unexpected behaviour might be the quality of the joints. From the metallographic investigations a comparatively steep flank angle can be identified for both specimen types, the fully penetration butt joint and the transverse stiffener. In addition, other individual specimen-characteristic influences such as an unconsidered angular misalignment might influence the fatigue life. In order to derive a reliable correlation between FAT-values and notch severity, further experiments should be performed with specimens with a low flank angle to broaden the data base.
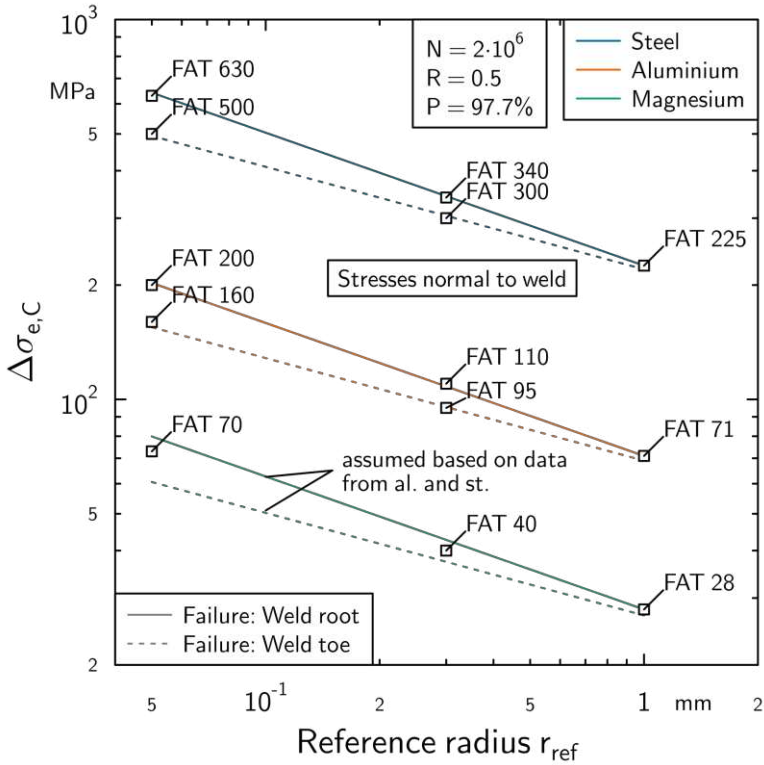

Figure 18: FAT-values for welded magnesium joints in dependence on the reference radius and the notch opening angle compared to data derived for aluminium and steel.

5. Conclusions

The present paper demonstrates the applicability of a fictitious notch radius, r_f, of 0.3 mm in local stress calculations for magnesium welded joints. $r_f = 0.3$ mm cannot be considered a definitive replacement for other fictitious notch radii (i.e., $r_f = 0.05$ mm and $r_f = 1.0$ mm). However, as demonstrated, $r_f = 0.3$ mm can be applied for specimens with thickness values between $3 \leq t \leq 10$ mm, with this allowing an adequate level of safety to be reached systematically. Additionally, based on the calculated local stresses, reference S-N curves are proposed for stress ratios R=-1, R=0 and R=0.5 which allowed us to identify appropriate FAT values according to the approach suggested in the IIW Recommendations. Based on the fictitious notch radius $r_f = 0.3$ mm, a FAT value was calculated as $\Delta\sigma_{FAT} = 40$ MPa at $N = 2 \times 10^6$.

Acknowledgements

References

[1] Radaj, D., Sonsino, C. M. and Fricke, W. *Fatigue assessment of welded joints by local approaches*. Woodhead publishing, 2006.

[2] Karakaş, Ö., Berto, F., and Susmel, L. (Editors). "Fatigue Assessment of Welded Joints by Modern Concepts." [Special issue] *International Journal of Fatigue* 101(2) (2017): 113-468.

[3] Atzori, B., Meneghetti, G., and Susmel, L. "Estimation of the fatigue strength of light alloy welds by an equivalent notch stress analysis." *International journal of fatigue* 24.5 (2002): 591-599.

[4] Susmel, L., and Tovo, R. "Local and structural multiaxial stress states in weldedjoints under fatigue loading." *International journal of fatigue* 28.5-6 (2006): 564-575.

[5] Susmel, L. "Modified Wöhler curve method, theory of critical distances and Eurocode 3: A novel engineering procedure to predict the lifetime of steel welded joints

subjected to both uniaxial and multiaxial fatigue loading." *International Journal of Fatigue* 30.5 (2008): 888-907.

[6]   Susmel, L. "The Modified Wöhler Curve Method calibrated by using standard fatigue curves and applied in conjunction with the Theory of Critical Distances to estimate fatigue lifetime of aluminium weldments." *International journal of fatigue* 31.1 (2009): 197-212.

[7]   Berto, F., Lazzarin, P., and Radaj, D. "Fictitious notch rounding concept applied to sharp V-notches: Evaluation of the microstructural support factor for different failure hypotheses. Part I: Basic Stress Equations". *Engineering Fracture Mechanics*, 75.10, (2008): 3060-3072.

[8]   Berto, F., Lazzarin, P., and Radaj, D. "Fictitious notch rounding concept applied to sharp V-notches: Evaluation of the microstructural support factor for different failure hypotheses. Part II: Microstructural support analysis." *Engineering Fracture Mechanics* 76.9 (2009): 1151-1175.

[9]   Radaj, D., Lazzarin, P., and Berto, F. "Generalised Neuber concept of fictitious notch rounding." *International Journal of Fatigue* 51 (2013): 105-115.

[10]   Berto, F., Lazzarin, P., and Radaj, D. "Fictitious notch rounding concept applied to V-notches with root holes subjected to in-plane shear loading." *Engineering Fracture Mechanics* 79 (2012): 281-294.

[11]   Berto, F., Lazzarin, P., and Radaj, D. "Fictitious notch rounding concept applied to V-notches with root hole subjected to in-plane mixed mode loading." *Engineering Fracture Mechanics* 128 (2014): 171-188.

[12]   Berto, F., Lazzarin, P., and Radaj, D. "Application of the fictitious notch rounding approach to notches with end-holes under mode 2 loading." *Structural Durability & Health Monitoring* 8.1 (2012): 31-44.

[13]   Remes, H., and Fricke, W. "Influencing factors on fatigue strength of welded thin plates based on structural stress assessment." *Welding in the World* 58.6 (2014): 915-923.

[14]   Fricke, W., Remes, H., Feltz, O., Lillemäe, I., Tchuindjang, D., Reinert, T., Nevierov, A., Sichermann, W., Brinkmann, M., Kontkanen, T., Bohlmann B., and Molter, L. "Fatigue strength of laser-welded thin-plate ship structures based on nominal and structural hot-spot stress approach." *Ships and Offshore Structures* 10.1 (2015): 39-44.

[15]   Pei, X., Wang, W., and Dong, P. "An Analytical-Based Structural Strain Method for Low Cycle Fatigue Evaluation of Girth-Welded Pipes." *ASME 2017 pressure vessels and piping conference*. American Society of Mechanical Engineers Digital Collection, 2017.

[16]   Pei, X., and Dong, P. "An analytically formulated structural strain method for fatigue evaluation of welded components incorporating nonlinear hardening effects." *Fatigue & Fracture of Engineering Materials & Structures* 42.1 (2019): 239-255.

[17]   Lazzarin, P., Berto, F., and Radaj, D. "Fatigue design of welded joints by local approaches: comparison between fictitious notch rounding and strain energy averaging." *Key Engineering Materials*. Vol. 348–349, Trans Tech Publications, Ltd., Sept. (2007): 449–452.

[18] Lazzarin, P., Berto, F., and Radaj, D. "Fatigue testing of welded joints by means of local criteria: a comparison between the fictitious notch radius–based criterion and the criterion involving strain energy density in a finite volume." *Welding International* 22.9 (2008): 635-640.

[19] Lazzarin, P., Berto, F., and Radaj, D."Fatigue-relevant stress field parameters of welded lap joints: pointed slit tip compared with keyhole notch." *Fatigue & Fracture of Engineering Materials & Structures* 32.9 (2009): 713-735.

[20] Radaj, D., Berto, F., and Lazzarin, P. "Local fatigue strength parameters for welded joints based on strain energy density with inclusion of small-size notches." *Engineering Fracture Mechanics* 76.8 (2009): 1109-1130.

[21] Radaj, D., Lazzarin, P., and Berto, F. "Fatigue assessment of welded joints under slit-parallel loading based on strain energy density or notch rounding." *International journal of fatigue* 31.10 (2009): 1490-1504.

[22] Radaj, D. "State-of-the-art review on extended stress intensity factor concepts." *Fatigue & Fracture of Engineering Materials & Structures* 37.1 (2014): 1-28.

[23] Berto, F., and Lazzarin, P. "Recent developments in brittle and quasi-brittle failure assessment of engineering materials by means of local approaches." *Materials Science and Engineering: R: Reports* 75 (2014): 1-48.

[24] Radaj, D. "State-of-the-art review on the local strain energy density concept and its relation to the J-integral and peak stress method." *Fatigue & Fracture of Engineering Materials & Structures* 38.1 (2015): 2-28.

[25] Hobbacher, A. *Recommendations for fatigue design of welded joints and components*. Springer, 2016.

[26] Zhang, G., Eibl, M., and Singh, S. "Methods of predicting the fatigue lives of laser-beam welded lap welds subjected to shear stresses." *Welding and cutting* 2 (2002): 96-103.

[27] Morgenstern, C., Sonsino, C. M., Hobbacher, A., and Sorbo, F."Fatigue design of aluminium welded joints by the local stress concept with the fictitious notch radius of rf= 1 mm." *International journal of fatigue* 28.8 (2006): 881-890.

[28] Eibl, M., and Sonsino, C. M. "Stand der Technik zur Schwingfestigkeitsberechnung von laserstrahl-geschweißten Dünnblechen aus Stahl." *Report* 668 (2001): 155-71.

[29] Eibl, M., Sonsino, C. M., Kaufmann, H., and Zhang, G. "Fatigue assessment of laser welded thin sheet aluminium." *International Journal of Fatigue* 25.8 (2003): 719-731.

[30] Schlemmer, J., Bacher-Höchst, M., and Sonsino, C. M. "Schwingfeste Auslegung von dünnwandigen Laserstrahlschweißverbindungen für Einspritzsysteme." *DVM-Bericht Nr.* 802 (2003): 25-36.

[31] Karakas, Ö., Morgenstern, C. and Sonsino, C. M. "Fatigue design of welded joints from the wrought magnesium alloy AZ31 by the local stress concept with the fictitious notch radii of rf= 1.0 and 0.05 mm." *International Journal of Fatigue* 30.12 (2008): 2210-2219.

[32] Karakas, Ö. "Consideration of mean-stress effects on fatigue life of welded magnesium joints by the application of the Smith–Watson–Topper and reference radius concepts." *International journal of fatigue* 49 (2013): 1-17.

[33] Susmel, L., Sonsino, C. M., and Tovo, R. "Accuracy of the Modified Wöhler Curve Method applied along with the rref= 1 mm concept in estimating lifetime of welded

joints subjected to multiaxial fatigue loading." *International journal of fatigue* 33.8 (2011): 1075-1091.

[34] Sonsino, C. M., Bruder, T., and Baumgartner, J. "SN lines for welded thin joints—suggested slopes and FAT values for applying the notch stress concept with various reference radii." *Welding in the World* 54.11-12 (2010): R375-R392.

[35] Störzel, K., Bruder, T., and Hanselka, H. "Durability of welded aluminium extrusion profiles and aluminium sheets in vehicle structures." *International Journal of Fatigue* 34.1 (2012): 76-85.

[36] Bruder, T., Störzel, K., Baumgartner, J., and Hanselka, H. "Evaluation of nominal and local stress based approaches for the fatigue assessment of seam welds." *International Journal of Fatigue* 34.1 (2012): 86-102.

[37] Hanssen, E., Vogt, M., and Dilger, K. "Fatigue assessment of arc welded automotive components using local stress approaches: application to a track control arm." *International Journal of Fatigue* 34.1 (2012): 57-64.

[38] Vogt, M., Dilger, K., & Kassner, M. "Investigations on different fatigue design concepts using the example of a welded crossbeam connection from the underframe of a steel railcar body." *International Journal of Fatigue* 34.1 (2012): 47-56.

[39] Baumgartner, J. "Review and considerations on the fatigue assessment of welded joints using reference radii." *International Journal of Fatigue* 101 (2017): 459-468.

[40] Karakaş, Ö. "Application of Neuber's effective stress method for the evaluation of the fatigue behaviour of magnesium welds." *International Journal of Fatigue* 101 (2017): 115-126.

[41] Karakaş, Ö., Zhang, G., and Sonsino, C. M. "Critical distance approach for the fatigue strength assessment of magnesium welded joints in contrast to Neuber's effective stress method." *International Journal of Fatigue* 112 (2018): 21-35.

[42] Neuber, H. "Über die Berücksichtigung der Spannungskonzentration bei Festigkeitsberechnungen." *Konstruktion* 20.7 (1968): 245-251.

[43] Peterson, R. E. "Notch Sensitivity, Metal Fatigue, Sines G., Waisman J. L." *New York: McGrawrHill* (1959).

[44] Taylor, D. "Geometrical effects in fatigue: a unifying theoretical model." *International Journal of Fatigue* 21.5 (1999): 413-420.

[45] Taylor, D. "The theory of critical distances." *Engineering Fracture Mechanics* 75.7 (2008): 1696-1705.

[46] Radaj, D. "Generalised Neuber concept of fictitious notch rounding." *Advanced Methods of Fatigue Assessment*. Springer, Berlin, Heidelberg, 2013. 1-100.

[47] Zhang, G., and Richter, B. "A new approach to the numerical fatigue-life prediction of spot-welded structures." *Fatigue & Fracture of Engineering Materials & Structures* 23.6 (2000): 499-508.

[48] Radaj, D., Sonsino, C. M., and Fricke, W. "Recent developments in local concepts of fatigue assessment of welded joints." *International Journal of Fatigue* 31.1 (2009): 2-11.

[49] Sonsino, C. M., Fricke, W., De Bruyne, F., Hoppe, A., Ahmadi, A., and Zhang, G. "Notch stress concepts for the fatigue assessment of welded joints–Background and applications." *International Journal of Fatigue* 34.1 (2012): 2-16.

[50] Karakas, Ö., Morgenstern, C., Sonsino, C. M., Hanselka, H., Vogt, H. M., and Dilger, K. "Grundlagen für die praktische Anwendung des Kerbspannungskonzeptes zur Schwingfestigkeitsbewertung von geschweißten Bauteilen aus Magnesiumknetlegierungen", Fraunhofer-Institut für Betriebsfestigkeit und Systemzuverlässigkeit LBF, Darmstadt, Bericht Nr." *FB-232* (2007).

[51] Exel, N., and Sonsino, C. M. "Multiaxial fatigue evaluation of laserbeam-welded magnesium joints according to IIW-fatigue design recommendations." *Welding in the World* 58.4 (2014): 539-545.

[52] Yung, J. Y., and Lawrence, F. V. "Analytical and graphical aids for the fatigue design of weldments." *Fatigue & Fracture of Engineering Materials & Structures* 8.3 (1985): 223-241.

[53] Anthes, R. J., Köttgen, V. B., and Seeger, T. "Kerbformzahlen von Stumpfstößen und Doppel-T-Stößen." *Schweißen und Schneiden* 45.12 (1993): 685-688.

[54] Lehrke, H. P., Brandt, U., and Sonsino, C. M. "Bruchmechanische Beschreibung der Wöhlerlinien geometrisch ähnlicher Schweißproben aus Aluminium." *Schweißen und Schneiden* 50.8 (1998): 492-497.

[55] Lehrke, H. P., Brandt, U., and Sonsino, C. M. "Berechnung von Formzahlen in Schweißverbindungen." *Konstruktion* 51.1/2 (1999): 47-52.

[56] Sonsino, C. M. "Course of SN-curves especially in the high-cycle fatigue regime with regard to component design and safety." *International Journal of Fatigue* 29.12 (2007): 2246-2258.

[57] Fricke, W. *IIW recommendations for the fatigue assessment of welded structures by notch stress analysis: IIW-2006-09*. Woodhead Publishing, 2012.